Sensors and Materials, Vol. 37, No. 8 (2025) 3465–3474
MYU Tokyo

S & M 4129

Design and Development of Off-grid Power Inverter

Cheng-Tao Tsai* and Jia-Wei Lin

Department of Electrical Engineering, National Chin-Yi University of Technology, Taichung 41170, Taiwan

(Received December 23, 2024; accepted June 18, 2025)

Keywords: off-grid, total harmonic distortion, sinusoidal pulse width modulation, peripheral interface controller

In this paper, an off-grid power inverter for the application of the photovoltaic (PV) power-generation system is proposed. The PV power-generation system used by an inverter supplies a utility sinusoidal source. To obtain the maximum power of the PV power-generation system and the low total harmonic distortion of the off-grid power inverter, a linear approximation control algorithm method and a sinusoidal pulse width modulation (SPWM) method are adopted. On the basis of an advanced control technology to obtain the optimum dynamic regulations of the off-grid power inverter, a peripheral interface controller and a SPWM microcontroller are used. Finally, to verify its feasibility, a prototype of the off-grid power inverter is built. Theoretical and experimental results are presented to demonstrate the performance of the off-grid inverter.

1. Introduction

Economic growth and industrial development are obvious to all in this century. Power energies will be a key point of economic growth and industrial development. Electricity generation using oil and gas results in carbon emissions. Solar photovoltaic (PV) energy has no carbon emissions, which is regarded as the most suitable energy conversion system.[1–3] However, solar PV energy needs to be converted to DC power using inverters. The PV system is an electric power system and is operated silently, which has evolved into a mature technology for mainstream electricity generation. Currently, the PV system can be categorized into various aspects, namely, grid-connected, standalone, residential and utility systems.[4–8]

Maximum power point tracking (MPPT) is a technique to obtain the maximum possible power from the PV system.[9–12] The intermittent power generation of PV panels results in rapidly changing voltage, which affects the power quality of the power inverter. Additionally, connecting to the grid poses many protection-related challenges. For example, island effects can be dangerous to electrical workers. In a standalone PV system, powers are insufficient to continuously supply the load. It usually needs a battery pack to supplement the power of the load. The standalone PV system is an independent unit, that is, does not rely on commercial powers when the powers of the PV system and battery sets are normally provided.[13–15] If both the PV system and the battery sets cannot provide normal power simultaneously, the commercial

*Corresponding author: e-mail: cttsai@ncut.edu.tw
https://doi.org/10.18494/SAM5522

ISSN 0914-4935

power (backup power) will provide powers to the load. To overcome the above disadvantages, an off-grid power inverter for the application of the PV system is used, as shown in Fig.1. The structure of the off-grid power inverter is described in Sect. 2. The principles of the linear MPPT are analyzed in Sect. 3. The experimental results used to verify the feasibility of the off-grid power inverter are shown in Sect. 4. Finally, the conclusions are given in Sect. 5.

2. Control Mechanism of MPPT

To obtain the maximum power utilization of PV panels, MPPT methods must be adopted. The published MPPT control algorithms of the PV system include the perturb-and-observe method, incremental conductance method, neural-network-based method, fuzzy-logic-control approach, and linear approximation method. Comparisons among these MPPT control algorithms show that the linear approximation method is the simplest. MPPT can be easily achieved using a linear curve to approximate the maximum power point of PV panels at different insolations.[16,17] Therefore, it can easily be realized in the PV system. The voltage–current (V–I) and power–voltage (P–V) characteristic curves of PV panels with different insolations are shown in Fig. 2. On the basis of the P–V characteristic curves, the equations in the output currents and powers of the PV panels can be expressed as

$$I_{pv} = I_{ph} - I_{sat}\left[\exp\left(\frac{q}{kTA}V_{pv}\right) - 1\right], \tag{1}$$

and

$$P_{pv} = I_{pv}V_{pv} = \frac{q}{kTA}I_{ph}\ln\left[\left(\frac{I_{ph}+I_{sat}-1}{I_{sat}}\right) - IR_s\right], \tag{2}$$

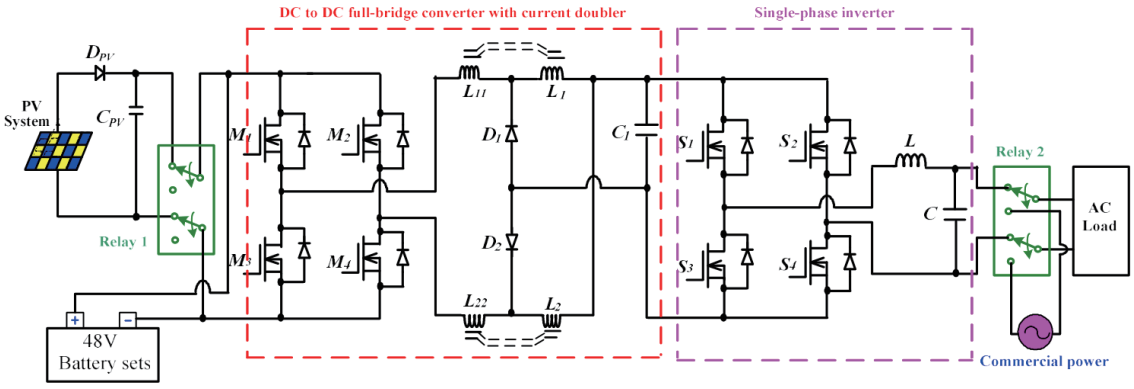

Fig. 1. (Color online) Circuit structure of an off-grid power inverter for application of PV power-generation system.

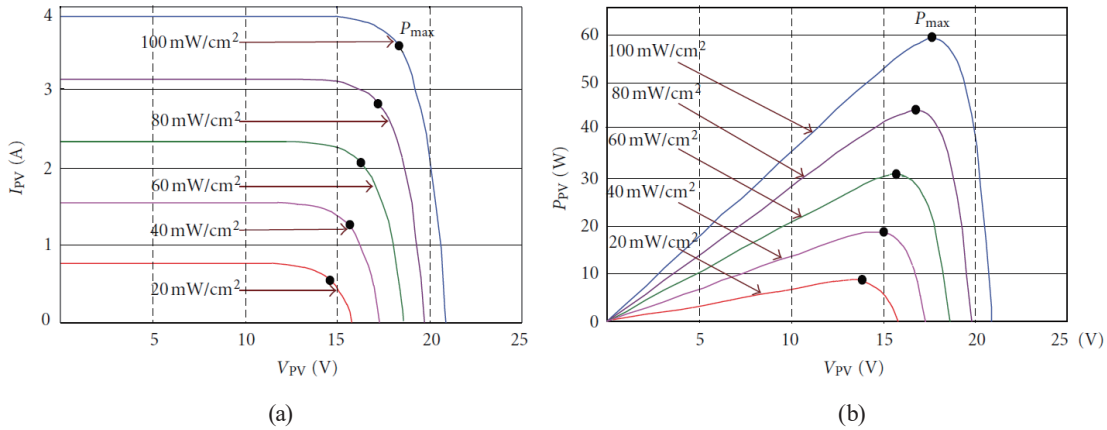

Fig. 2. (Color online) PV panels operated at different insolations: (a) V–I and (b) P–V curves.

where I_{sat} is the reverse-saturation current, I_{ph} is the output current, R_s is the series resistance of the PV panels, q denotes the charge of an electron (1.6×10^{-19} coulomb), and k is the Boltzmann's constant (1.38×10^{-23}J/° K) of the PV panels. From Eqs. (1) and (2), we can obtain the linear approximation curve of the maximum power P_{pv} and the output current I_{pv} curve, as shown in Fig. 3. The linear approximation control algorithms of MPPT are integrated in a peripheral interface controller, the PIC16F1824 microprocessor.

3. Structure of Off-grid Power Inverter

The proposed off-grid power inverter consists of a PV power-generation system, battery sets, a DC full-bridge converter, and a single-phase inverter, as shown in Fig. 1. Under normal sunlight, the PV energy stored in battery sets is supplied to a full-bridge converter simultaneously. Input voltages of 48 V_{DC} via the full-bridge converter can boost DC voltages to a higher level of 200 V_{DC}. Then, the single-phase inverter converts voltages of 200 V_{DC} to AC 110 V_{rms} for the AC load. When the PV system and battery sets cannot simultaneously provide normal power to the AC load, the off-grid power inverter will enter the operation mode of the commercial power to provide the powers of the AC load.

The off-grid power inverter is composed of two parts: a power stage and a control stage. The power stage includes a DC step-up circuit for a full-bridge converter and a DC-to-AC circuit for a single-phase inverter. The control stage includes control circuits of MPPT and power relay sets.

3.1 Description of DC-to-AC power stage

To supply AC power, the low DC voltages need a step-up circuit to boost the output voltages of PV panels and battery sets. Then, the boosted DC voltages are converted into AC power by an inverter circuit. In this study, a full-bridge converter combining a single-phase inverter is adopted. The full-bridge converter has the following advantages: (1) it uses a high-frequency transformer, with safety functions of electrical isolation, (2) it adjusts the turns ratio of the high-

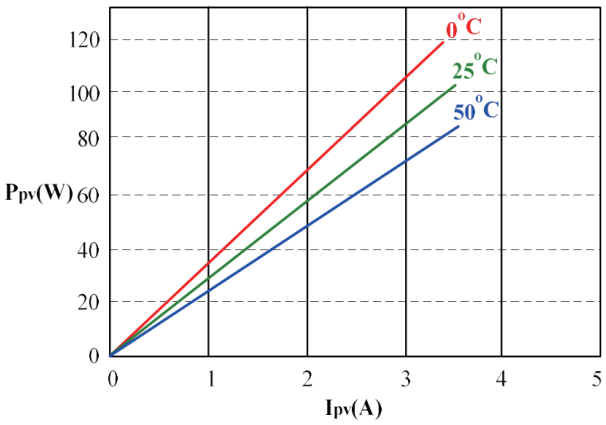

Fig. 3. (Color online) Maximum power and output current curves of PV panels.

frequency transformer, that is, high output voltages of the full-bridge converter can be easily obtained, (3) the output terminal of the full-bridge converter is connected to a current-doubler rectifier, which can obtain low-output-current ripples, and (4) it uses a phase-shift controller to realize the soft switching of power switches, which can obtain high conversion efficiency. To obtain small current harmonics and the best dynamic regulation of AC output powers, a unipolar sinusoidal pulse width modulation (SPWM) controller and an output filter are adopted. The output filter is a second-order low-pass circuit, which is composed of an inductor (L) and a capacitor (C), as shown in Fig. 4. To eliminate output AC current noise, the resonant frequencies of L and C must conform to the following equations:

$$10 f_o \le \frac{1}{2\pi\sqrt{LC}} \le \frac{f_s}{10}, \tag{3}$$

where f_o is the fundamental frequency of sinusoidal waves and f_s is the switching frequency. Additionally, by the unipolar SPWM control method, the design values of L and C must meet the following conditions:

$$L \ge \frac{V_L T_s}{2 i_{L-peak}}, \tag{4}$$

and

$$C \ge \frac{0.25 i_{L-peak} T_s}{2 V_{o(rms)}(0.5\%)}, \tag{5}$$

where V_L is the voltage of L, T_s is the switching period, $i_{L\text{-}peak}$ is the peak current of L, and $V_{o(rms)}$ is the root-mean-square value of AC output voltages. According to Eqs. (3)–(5), small current harmonics and the best dynamic regulation of AC output powers can be obtained. The circuit structure of the DC-to-AC power stage is shown in Fig. 5.

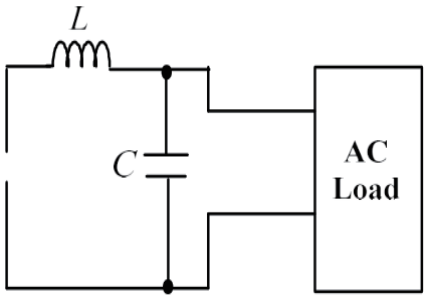

Fig. 4. Structure of LC filter.

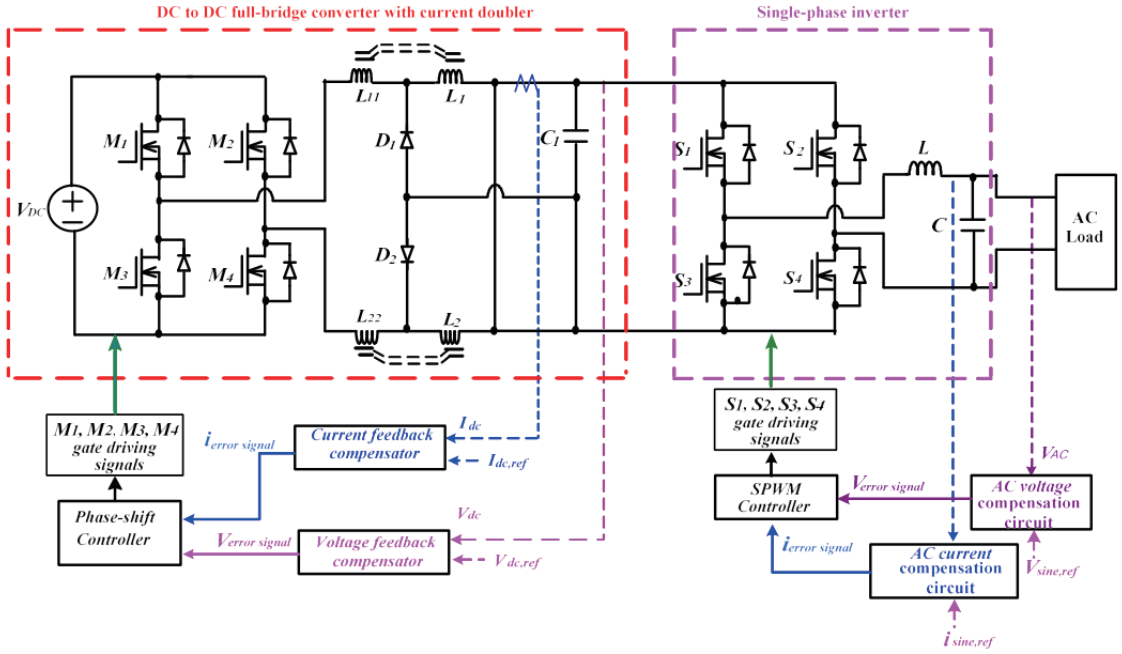

Fig. 5. (Color online) Circuit structure of DC-to-AC power stage.

3.2 Description of PV power-generation system and utility

Figure 6 shows the control structure of the PV power-generation system and utility. The PV power-generation system not only provides power to the single-phase inverter, but also stores excess power in the battery sets. When the power of the PV power-generation system is insufficient, the stored power of the battery sets is provided to the AC load by turning on Relay 1. If both the powers of the PV power-generation system and battery sets are simultaneously insufficient, commercial power will be provided to the AC load by turning on Relay 2. The under-power status of the PV power-generation system and battery sets is detected by the PIC16F1824 microprocessor.

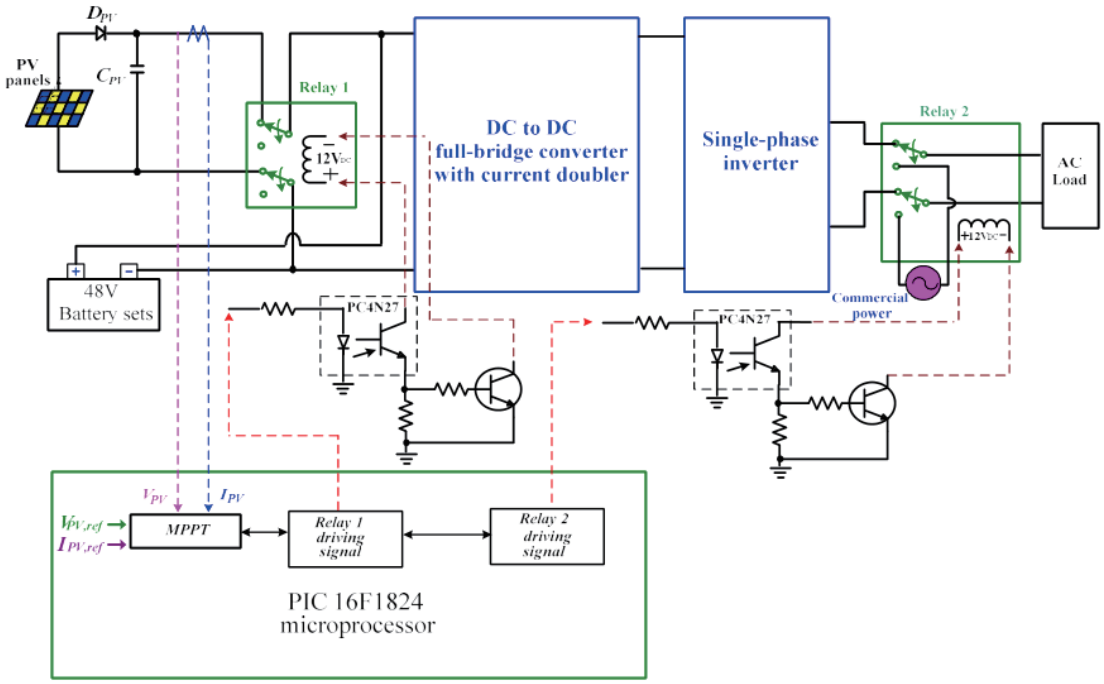

Fig. 6. (Color online) Control structure of PV power-generation system and commercial power.

4. Experimental Results

To verify the performance of the off-grid power inverter for the application of the PV power-generation system, we built a test apparatus of the PV power-generation system to produce the output AC powers. Its specifications are as follows:

※ output voltage of PV power-generation system: $V_{PV} = 52\ V_{DC}$,
※ voltage of battery sets: $V_{bat} = 48\ V_{DC}$,
※ DC output voltage of full-bridge converter: $V_{DC} = 200\ V_{DC}$,
※ output AC voltage of single-phase inverter: $V_{AC} = 110\ V_{AC}$, 60 Hz, and
※ output power of single-phase inverter: $P_{o,max} = 1.1$ KW.

Figure 7 shows the output voltage and current waveforms of the single-phase inverter measured with SPWM technologies, which shows that the output voltage and current waves forms are in phase under the full load condition. Figure 8 shows that the single-phase inverter with SPWM technologies can obtain the best pure sinusoidal powers. From the above measurement results, we verified that the single-phase inverter can obtain a low total harmonic distortion (THD) and a high power factor. Figure 9 shows the measured turn-on and turn-off waveforms of Relays 1 and 2, which shows that when the PV power-generation system and battery power are insufficient, the load power is provided by commercial power. Relay 1 is turned off and Relay 2 is turned on. Figure 10 shows the driving signals of switches (S_1, S_2, S_3 and S_4), which shows that switches S_2 and S_4 are operated at a low frequency (60 Hz), and switches S_1 and S_3 are operated at a high frequency (400 kHz). Figure 11 shows the measured current and voltage of the LC filter.

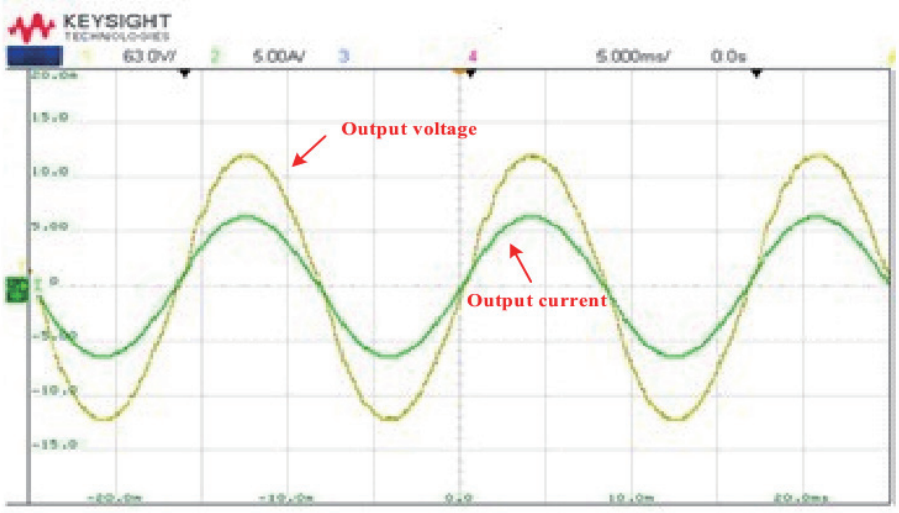

Fig. 7. (Color online) Measured output voltage and current waveforms of single-phase inverter.

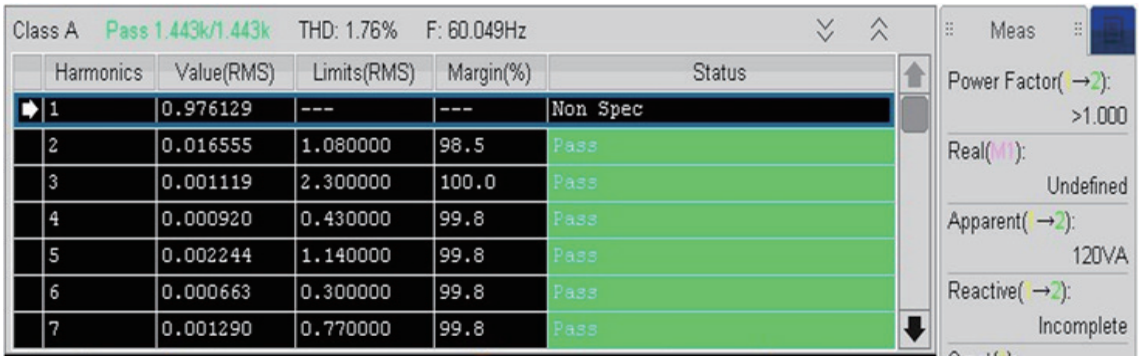

Fig. 8. (Color online) Measured THD and power factor of single-phase inverter.

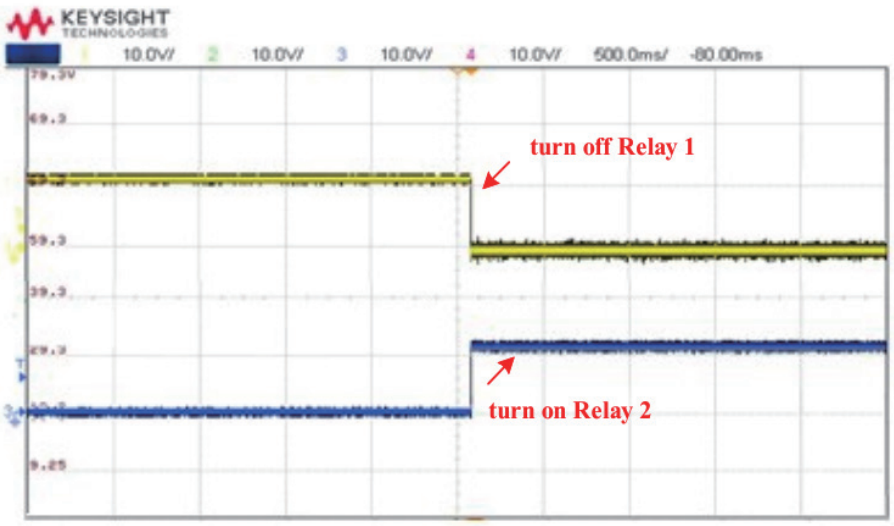

Fig. 9. (Color online) When the commercial power provided the load power, turn off Relay 1 and turn on Relay 2.

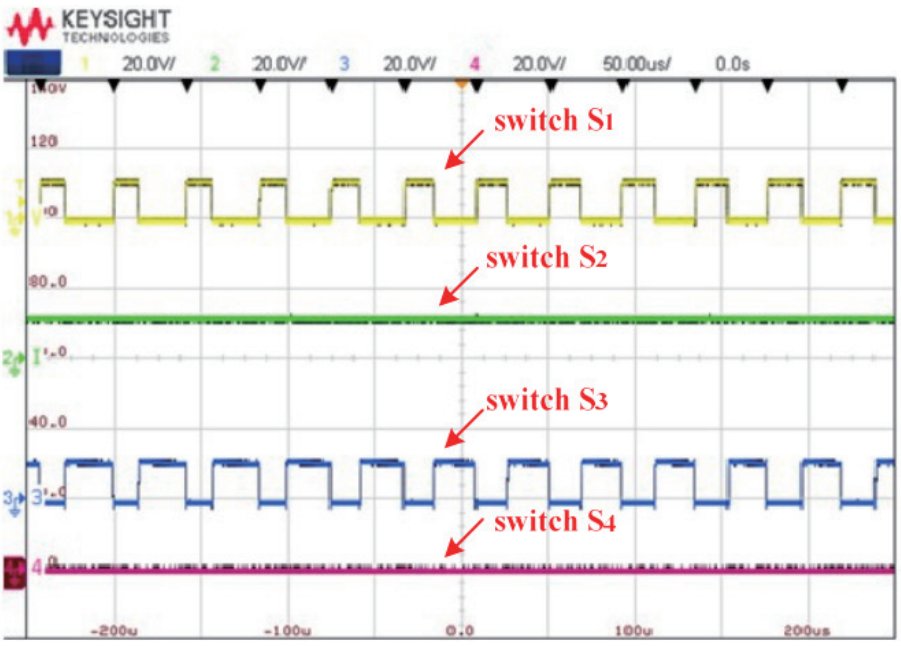

Fig. 10. (Color online) Measured driving signals of switches (S1, S2, S3 and S4).

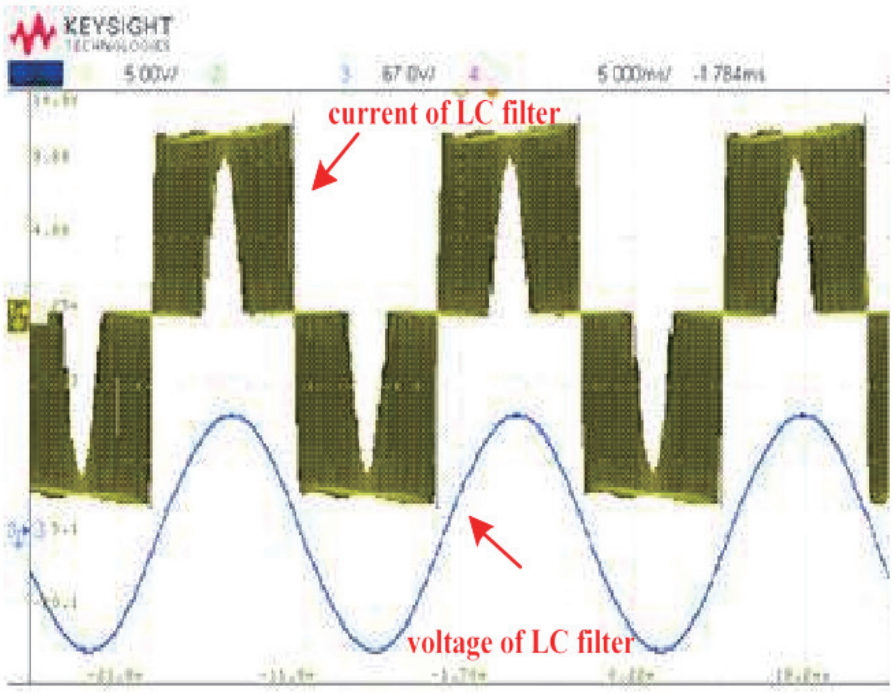

Fig. 11. (Color online) Measured current and voltage waveforms of LC filter.

5. Conclusions

An off-grid power inverter for the application of the PV power-generation system was built and implemented. It consists of a PV power-generation system, a DC–DC full-bridge converter and an SPWM power inverter to generate AC sinusoidal power. From the experimental results, the off-grid power inverter can obtain a low THD and a high power factor. To obtain the maximum power of the PV power-generation system, a linear approximation method was used by the PIC16F1824 microprocessor to implement MPPT to obtain the maximum power transmission. The design and development of the off-grid power inverter were implemented. The experimental results showed that the THD is 1.76%, which matches the THD in the EEE standard.

Acknowledgments

This work was supported by National Chin-Yi University of Technology, Taiwan

Author Contributions

Cheng-Tao Tsai designed the circuit and wrote this paper, and Jia-Wei Lin contributed to obtaining the experimental results.

Conflicts of Interests

The authors declare that there are no conflicts of interest regarding the publication of this paper.

References

1 S. Kouro, J. Rebolledo, and J. Rodríguez: IEEE Trans. Ind. Electron. **54** (2007) 2894. https://doi.org/10.1109/TIE.2007.905968
2 C. Koroneos, T. Spachos, and N. Moussiopoulos: Renewable Energy **28** (2003) 295. https://doi.org/10.1016/S0960-1481(01)00125-2
3 J. Cao, N. Schofield, and A. Emadi: Proc. IEEE Vehicle Power and Propulsion Conf. (IEEE, 2008) 11058. https://doi.org/10.1109/VPPC.2008.4677669
4 K. Taesic and Q. Wei: IEEE Trans. Energy Convers. **26** (2011) 1172. https://doi.org/10.1109/TEC.2011.2167014
5 E. J. Lee and K. B. Lee: J. Power Electron. **21** (2021) 541. https://doi.org/10.1007/s43236-020-00200-w
6 J. Amini and M. Moallem: IEEE Trans. Ind. Electron. **64** (2017) 1818. https://doi.org/10.1109/TIE.2016.2624722
7 K. W. E. Cheng, B. P. Divakar, H. Wu, K. Ding, and H. F. Ho: IEEE Trans. Vehicular Technol. **60** (2010) 76. https://doi.org/10.1109/TVT.2010.2089647
8 J. Zhang, D. D.-C. Lu, and T. Sun: IEEE Trans. Ind. Electron. **57** (2010) 1041. https://doi.org/10.1109/TIE.2009.2028336
9 S. M. Chen, T. J. Liang, L. S. Yang, and J. F. Chen: IEEE Trans. Power Electron. **26** (2011) 1146. https://doi.org/10.1109/TPEL.2010.2090362
10 M. Ceraolo and G. Pede: IEEE Trans. Vehicular Technol. **50** (2001) 109. https://doi.org/10.1109/25.917893
11 S. Shi, X. Wang, S. Zheng, Y. Zhang, and D. Lu: IEEE Trans. Ener. Conv. **33** (2018) 2220. https://doi.org/10.1109/TEC.2018.2863561
12 M. D. Siddique, S. Mekhilef, N. M. Shah, J. S. M. Ali, and F. Blaabjerg: IEEE Trans. Circ. and Syst. **53** (2020) 1294. https://doi.org/10.1109/TCSII.2019.2932480

13 I. Batarseh: IEEE Trans. Power Electron. **9** (1994) 64. https://doi.org/10.1109/63.285495
14 R. L. Steigerwald: IEEE Trans. Power Electron. **3** (1988) 174. https://doi.org/10.1109/63.4347
15 H. P. Park and J. H. Jung: Ind. Electron. **64** (2016) 253. https://doi.org/10.1109/TIE.2016.2599138
16 W. Hao, J. Gong, X. Zhao, C. S. Yeh, and J. S. Lai: IEEJ Trans. Power Electron. **34** (2019) 11952. https://doi.org/10.1109/TPEL.2019.2909426
17 K. Kobayashi, H. Matsuo, and Y. Sekine: IEEE Trans. Ind. Electron. **53** (2006) 281. https://doi.org/10.1109/TIE.2005.862250